

## Article

# Replacing Fly Ash or Silica Fume with Tuff Powder for Concrete Engineering in Plateau Areas: Hydration Mechanism and Feasibility Study

Tianqi Li <sup>1,2</sup>, Bixiong Li <sup>1,2,\*</sup>, Lianghui Li <sup>1,2</sup> , Zhiwen Wang <sup>1,2</sup>, Zhibo Zhang <sup>1,2</sup> and Qingshun Nong <sup>1,2</sup>

- <sup>1</sup> College of Architecture and Environment, Sichuan University, Chengdu 610065, China; lisichuan1@hotmail.com (T.L.); lilianghuisichuan@163.com (L.L.); wangzhiwenmail@163.com (Z.W.); zhangzhibomail@163.com (Z.Z.); cengseonnung@foxmail.com (Q.N.)
- <sup>2</sup> Key Laboratory of Deep Earth Science and Engineering Ministry of Education, Sichuan University, Chengdu 610065, China
- \* Correspondence: libix@scu.edu.cn

**Abstract:** Abundant tuff mineral resources offer a promising solution to the shortage of fly ash (FA) and silica fume (SF) resources as emerging supplementary cementitious materials. However, a lack of clarity on its hydration mechanism has hindered its practical engineering application. In this study, high SiO<sub>2</sub>-content tuff powder (TP) was examined to assess the mechanical and workability performance of mortar specimens with varying particle sizes of the TP as complete replacements for FA or SF. Microscopic analysis techniques, including X-ray diffraction (XRD), differential thermal analysis (DTG), and energy-dispersive X-ray spectroscopy (EDS), were employed to elucidate the hydration mechanism of the TP and its feasibility as a substitute for SF or FA. Results indicated that TP primarily functions as nuclei and filler, promoting cement hydration, with smaller particle sizes amplifying the hydration ability and increasing Ca(OH)<sub>2</sub> and C-S-H gel content. The specimens with TP (median particle size 7.58 μm) demonstrated 9.2% and 29.9% higher flexural and compressive strengths at 28 days, respectively, compared to the FA specimens of equal mass. However, fluidity decreased by 23.1% accordingly. Due to TP's smaller specific surface area compared to SF, the TP specimens exhibited higher fluidity but with decreased strength relative to the SF specimens. Overall, TP shows potential as a replacement for FA with additional measures to ensure workability.

**Keywords:** tuff powder; fly ash; silica fume; phase analysis; calcium/silicon ratio



**Citation:** Li, T.; Li, B.; Li, L.; Wang, Z.; Zhang, Z.; Nong, Q. Replacing Fly Ash or Silica Fume with Tuff Powder for Concrete Engineering in Plateau Areas: Hydration Mechanism and Feasibility Study. *Buildings* **2024**, *14*, 1232. <https://doi.org/10.3390/buildings14051232>

Academic Editor: Grzegorz Ludwik Golewski

Received: 25 March 2024

Revised: 17 April 2024

Accepted: 24 April 2024

Published: 26 April 2024



**Copyright:** © 2024 by the authors. Licensee MDPI, Basel, Switzerland. This article is an open access article distributed under the terms and conditions of the Creative Commons Attribution (CC BY) license (<https://creativecommons.org/licenses/by/4.0/>).

## 1. Introduction

Cement, as one of the raw materials for concrete production, emits a significant amount of greenhouse gases such as carbon dioxide during its transportation and manufacturing processes [1], thereby causing severe pollution to the atmospheric environment. To reduce carbon emissions in construction projects, it is imperative to minimize transportation distances and, more importantly, reduce the use of cement by incorporating common mineral admixtures such as fly ash and silica fume into concrete to achieve the goal of reducing cement consumption. However, with the widespread use of fly ash, the global community is facing a shortage of this resource [2,3]. Additionally, in high-altitude regions such as La Concordance in Peru, Karaoke in India, and Tibet in China, the transportation costs of common mineral admixtures like fly ash or silica fume are considerably high. Therefore, the search for widely distributed new mineral admixtures has become a pressing priority [4].

In plateau regions, common natural volcanic ash materials include tuff, pumice, zeolite, and diatomaceous earth [5], among which tuff has the most widespread distribution worldwide. Tuff is a suitable mineral admixture for substituting fly ash and silica fume in plateau regions. Tuff is formed from volcanic eruption debris through compaction

and chemical bonding from hydration reactions. It possesses a highly porous structure, high surface area, and low density, with main minerals including quartz, feldspar, clay, and zeolite [6]. Tuff rock powder displays a fragmental structure, distinct edges, and irregular shapes. Consequently, concrete with tuff powder requires a higher unit water content, necessitating prolonged mixing times during the blending process and enhanced vibration and compaction during pouring to ensure concrete quality [7–9]. The inclusion of tuff powder enhances concrete crack resistance and deformability [10]. In recent years, tuff powder has been successfully employed in hydraulic engineering. For instance, the Manwan Hydropower Station and the Dachaoshan Hydropower Station in the middle reaches of the Lancang River utilized tuff powder as an auxiliary cementitious material in dam concrete. This not only reduces transportation costs but also effectively enhances the crack resistance of concrete, simplifies temperature control measures, and accelerates construction progress [11].

Due to the different geological environments, the composition and structure of tuff in various regions can vary significantly, leading to variations in the impact of tuff powder on the mechanical properties of cement-based composite materials as reported in existing studies. Çavdar [12] found that the activity of tuff powder is directly proportional to compressive strength and  $\text{SiO}_2$  content. Kunal et al. [13,14] discovered that a higher  $\text{SiO}_2$  content in tuff powder results in a more pronounced pozzolanic effect, which favors the early development of compressive strength in tuff powder–silicate cement-based materials. However, other studies [9,15] have indicated that the inclusion of tuff powder may lead to varying degrees of reduction in the mechanical properties of concrete, possibly due to the lower  $\text{SiO}_2$  content in the tuff powder used in these experiments.

Moreover, since the hydration mechanism of tuff powder remains unclear, there are contrasting views regarding its impact on the setting time of concrete. Turanlı [16,17] found that both the initial and final setting times of the composite cementitious systems with tuff powder were longer than those with pure cement, and the setting time increased with the amount of tuff powder added. In contrast, Li [18] revealed that the initial and final setting times of the composite cementitious systems with 30% tuff powder were shortened, attributing this to the nucleation effect and pozzolanic reaction of tuff powder, thus accelerating the  $\text{C}_3\text{S}$  hydration rate and shortening the setting time. Understanding the hydration mechanism of tuff powder is crucial to validate its feasibility as a reliable mineral admixture. Recently the Gaozheng Building Materials Company found tuff with high  $\text{SiO}_2$  content in Tibet. If this tuff powder can be used as admixture instead of fly ash or silica fume, then the cost of concrete construction in plateau area can be greatly reduced.

Currently, research on the hydration mechanism of tuff powder with high  $\text{SiO}_2$  content is limited, and whether this kind of tuff powder can replace or partially substitute fly ash or silica fume remains unknown. Therefore, this study focuses on high  $\text{SiO}_2$ -content tuff powder, comparing it with fly ash and silica fume. Through testing flexural and compressive strength and workability, combined with microscopic techniques such as X-ray diffraction (XRD), differential thermal analysis (DTG), and energy-dispersive spectroscopy (EDS), we investigate the strength effects and hydration mechanisms of tuff powder at different fineness levels in cementitious materials. Our research aims to establish a theoretical foundation for the promotion and application of tuff powder and provide guidance for its future application in concrete engineering.

## 2. Materials

The cement used was the reference cement produced by the Aoser Company in Fushun city, Liaoning Province, China, and met the quality requirements of the government standard GB 8076-2008 [19] for reference cement. Its technical indicators are shown in Table 1. The fly ash (FA) used was the first-class fly ash produced by the Borun Company in Henan Province, China. The tuff powder (TP) used was the tuff powder mined and processed by the Gaozheng Building Materials Company in Xizang Province, China. The coarse particle-sized tuff powder (CT) used was obtained by passing the broken tuff

through a 300-mesh sieve; the medium particle-sized tuff powder (MT) used was obtained by grinding by the Gaozheng Building Materials Company in Xizang Province, China.; the fine particle-sized tuff (FT) used was obtained by grinding the MT with a ball mill for 3 h. The appearance of the tuff powders with the three different particle sizes is shown in Figure 1, and the technical indicators are shown in Table 2. The microscopic morphology of the CT is shown in Figure 2. The silica fume (SF) used was produced by the IMERYS Company in British. The fine aggregate used was standard sand produced by the ISO Standard Sand Company in Xiamen city, Fujian Province, China. The chemical composition of the cement, fly ash, silica fume, and tuff powder used was obtained through X-ray fluorescence (XRF) analysis, as shown in Table 3. The particle size distribution was obtained through a laser particle size analyzer, as shown in Table 4 and Figure 3. The phase analysis results obtained through X-ray diffraction are shown in Figure 4.

**Table 1.** Reference cement technical indicators.

Density (g/cm <sup>3</sup> )	Normal Consistency (%)	Specific Surface Area (m <sup>2</sup> /kg)	Initial Setting Time (min)	Final Setting Time (min)	Stability	Flexural Strength (MPa)	Compressive Strength (MPa)
3.16	26.6	358	128	196	Qualified	5.3	26



**Figure 1.** Three different particle sizes of tuff powder (a) CT, (b) MT, and (c) FT.

**Table 2.** Physical properties of three groups of tuff powder.

Materials	Density (g/cm <sup>3</sup> )	Specific Surface Area (m <sup>2</sup> /g)	Water Demand Ratio (%)	28d Activity Index (%)	Moisture Content (%)	Stability
FT	2.48	23.42	113	104.7	0.41	Qualified
MT	2.48	11.13	108	91.2	0.22	Qualified
CT	2.48	5.02	105	73.4	0.16	Qualified

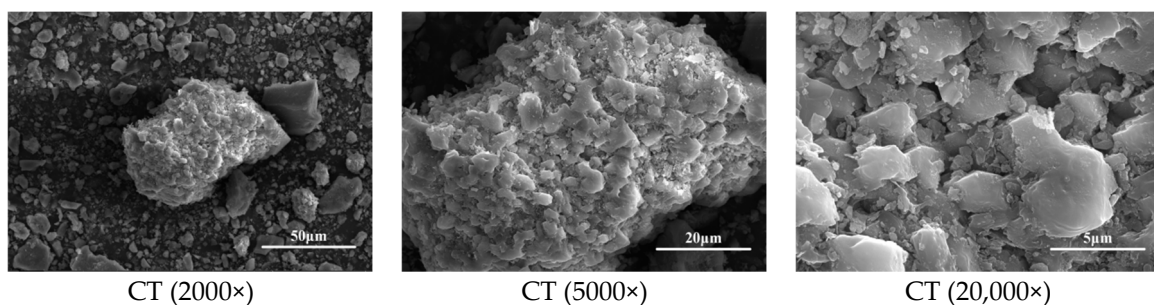


**Figure 2.** SEM images of CT.

**Table 3.** Chemical composition of cement, fly ash, silica fume, and tuff powder (wt%).

Materials	SiO <sub>2</sub>	Na <sub>2</sub> O	K <sub>2</sub> O	Al <sub>2</sub> O <sub>3</sub>	CaO	Fe <sub>2</sub> O <sub>3</sub>	MgO	SO <sub>3</sub>	LOI
Cement	22.81	0.53	0	4.11	63.22	3.16	3.19	2.08	0.9
Fly ash	56.41	0.12	1.79	24.2	7.1	7.98	0.35	1.2	0.85
Silica fume	96.5	0.37	0.76	0.34	0.4	0.07	0.8	0.28	0.48
Tuff powder	94.0	0.05	0.08	0.67	0.579	1.50	0	2.76	0.36

**Table 4.** Particle size distribution of cement, fly ash, silica fume, and tuff powder (µm).

Particle Size	Cement	Fly Ash	Silica Fume	FT	MT	CT
D10	3.17	2.52	0.03	1.66	1.88	2.07
D50	17.79	14.31	0.48	7.58	12.86	24.97
D90	48.89	89.38	2.22	32.33	56.64	79.3

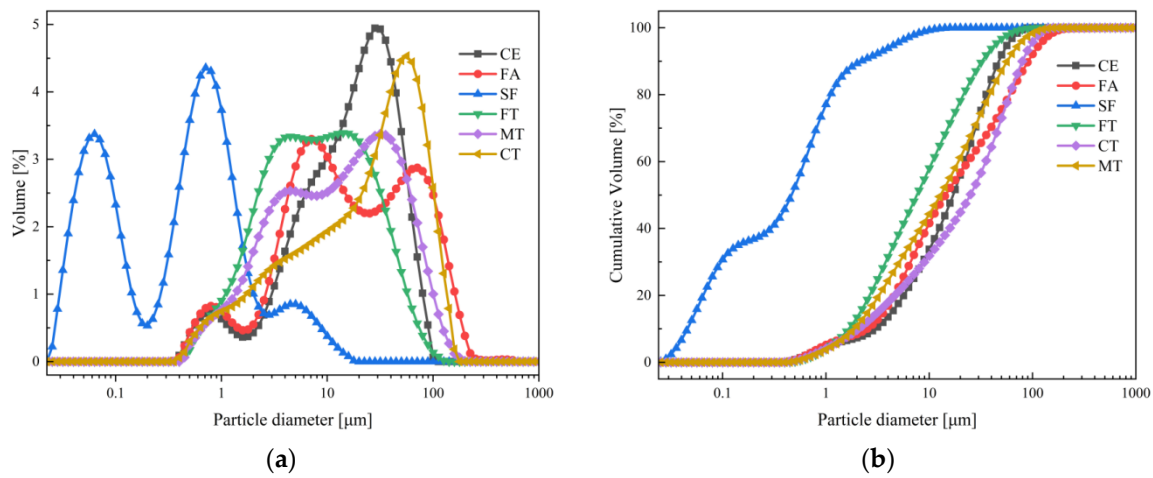


**Figure 3.** Particle size distributions of cement, fly ash, silica fume, FT, MT, and CT. (a) Particle size distribution; (b) accumulated particle size pass rate.

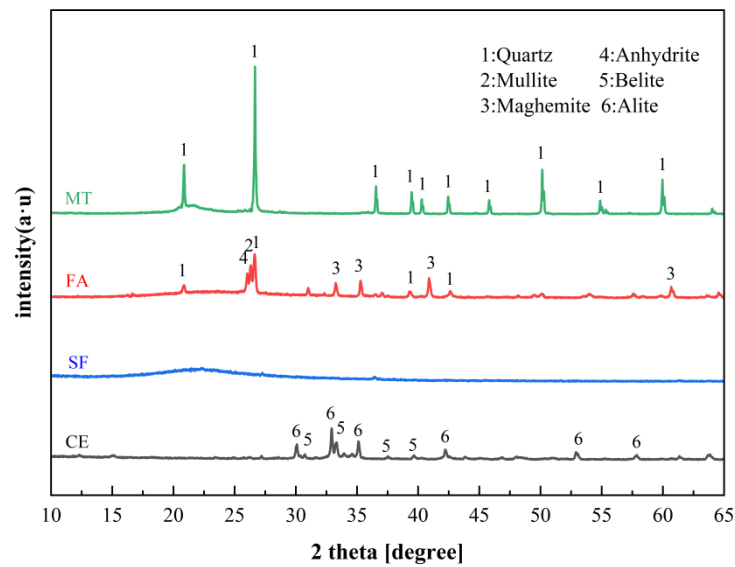


**Figure 4.** Phase composition of cement, fly ash, silica fume, and tuff powder.

2.1. Experimental Designs

In order to study the influence of the different fineness of the tuff powder on the strength of the cement mortar, the hydration mechanism of the tuff powder in cementitious

materials, and the feasibility of replacing fly ash or silica fume with the tuff powder, the experiment mix proportion was designed according to the industrial standard JB/T 315-2011 [20] and government standard GB/T 27690-2023 [21]. The experimental mix proportions are shown in Tables 5 and 6. FA30, FT30, MT30, and CT30 are mortar specimens that replaced 30% cement with FA, FT, MT, and CT, respectively; SF10, FT10, MT10, and CT10 are mortar specimens that replaced 10% cement with SF, FT, MT, and CT, respectively.

**Table 5.** The mix proportion design of the feasibility study of replacing fly ash with tuff powder (g).

Group Number	Cement	Fly Ash	Tuff Powder	Standard Sand	Water
JZ-1	450	0	0	1350	225
FA30	315	135	0	1350	225
FT30	315	0	135 (fine)	1350	225
MT30	315	0	135 (middle)	1350	225
CT30	315	0	135 (coarse)	1350	225

**Table 6.** The mix proportion design of the feasibility study of replacing silica fume with tuff powder (g).

Group Number	Cement	Silica Fume	Tuff Powder	Standard Sand	Water
JZ-2	450	0	0	1350	225
SF10	405	45	0	1350	225
FT10	405	0	45 (fine)	1350	225
MT10	405	0	45 (middle)	1350	225
CT10	405	0	45 (coarse)	1350	225

## 2.2. Experimental Methods

### 2.2.1. Specimen Preparation and Curing Methods

The mixing, forming, vibrating, and demolding of the cement mortar were carried out according to GB/T 17671-2021 [22]. JZ-1, FA30, FT30, MT30, and CT30 were put into the standard curing room for 3 days, 7 days, and 28 days. JZ-2, SF10, FT10, MT10, and CT10 were put into the 60 °C steam-curing box for 3 days, 7 days, and 28 days.

### 2.2.2. Strength and Fluidity Tests

After curing the specimen to the specified age (3d, 7d, and 28d), the strength tests were carried out. The flexural and compressive strength tests were carried out according to the government standard GB/T 17671-2021 [22]. The water–binder ratio of all the specimens was 0.5 without a water-reducing agent. The specific operation method of the fluidity test referred to the government standard GB/T 2419-2005 [23].

### 2.2.3. The 28 d Activity Index Test and Water Demand Ratio Test

The 28 d activity index is an important index to evaluate the strength of pozzolanic materials, which is obtained by dividing the compressive strength of the experimental group by that of the base group. The experimental groups were made of the tuff powder with different particle sizes instead of the 30% cement, and the 28 d compressive strength of the tuff powder with different particle sizes was measured, respectively, after 28 d standard curing, and then the 28 d activity indexes of the tuff powder with different particle sizes were obtained by dividing the 28 d compressive strength of the base group, respectively. Water demand ratio is an important index to evaluate the quality of volcanic ash material and their engineering application. With 250 g reference cement, 750 g intermediate sand, and 125 g water, the standard sand glue was configured and its fluidity was measured. With 175 g reference cement, 75 g tuff powder, 750 g intermediate sand, and some water the experimental sand glue was configured and its fluidity was measured. The water consumption of the experimental sand glue was adjusted to change its fluidity. When the fluidity of the experimental sand glue was consistent with the benchmark sand glue, the

water consumption of the experimental sand glue at this time was recorded. The water demand ratio of the tuff powder was calculated by dividing the water consumption of the experimental sand glue by 125 g.

#### 2.2.4. XRD Test and DTG Test

After 28 days of curing, the specimen was crushed and small pieces were taken out, and then they were put into a small bottle filled with anhydrous ethanol to stop hydration. The duration was about 2 days, and then they were put into a drying box. After drying the moisture in the drying box, they were ground into a powder with a grinding rod and screened with a 200-mesh sieve [24]. The sifted powder was tested by XRD and DTG. Bruker D8 advance equipment was selected for the XRD test, a copper target was used, the diffraction angle was 5–90 degrees, and the scanning speed was 10°/min. After obtaining the diffraction peak data, Jade6.5 software was used for phase analysis. During the DTG test, Mettler TGA2 type equipment was selected, the heating range was 20 to 1000 °C, the heating rate was 10 °C/min, and nitrogen was used as the protective gas.

#### 2.2.5. EDS Spectrum Test

The EDS spectrometer can be used for the elemental material analysis of the specimen, which can generally be combined with scanning electron microscopy or transmission electron microscopy. The principle is to maintain a vacuum environment, where the specimen is bombarded with characteristic rays with an electron beam, and the elements can be analyzed according to their wavelengths. A small piece with a diameter of no more than 10mm was taken from the middle of the specimen and placed in anhydrous ethanol for 2 days to achieve the purpose of stopping hydration. The moisture in the small piece was dried by the drying box, and then the small piece was sent to the testing unit for EDS testing. The content of O, Mg, Al, Si, K, and Ca elements in the fixed area was tested by point scanning, and the hydration of the specimen was analyzed by element content.

### 3. Test Results

#### 3.1. Flexural Strength and Compressive Strength

The flexural strength and compressive strength of the cement mortar in the fly ash comparison group and the silica fume comparison group at different curing times are shown in Figures 5 and 6, respectively. As can be seen from Figure 5a, for the flexural strength, the FA30, FT30, MT30, and CT30 groups were lower than the JZ-1 group at 3 days, and there was little difference between the FT30 group and the JZ-1 group at 28 days while the FT30 group was higher than the FA30 group at 3 days. On the contrary, the MT30 group was higher than the FA30 group only at 3 days and 7 days, and lower than the FA30 group at 28 days. The CT30 group was lower than the FA30 group. As can be seen from Figure 5b, for the compressive strength, the early strength of the FA30, FT30, MT30, and CT30 groups were lower than that of the JZ-1 group, but the strength of the FT30 and MT30 groups increased significantly in the middle curing period, making the strength of the FT30 group higher than that of the JZ-1 group and the strength of the MT30 group slightly lower than that of the JZ-1 group at 28 days. The FA30 group was much lower than the FT30 and MT30 group in the middle and late curing periods. By comparison, it can be seen that the effect of the tuff powder on the flexural strength of the cement mortar is lower than that of the fly ash, but the effect on the compressive strength of the cement mortar is much greater than that of the fly ash. It can be seen from Figure 6 that the FT10, MT10 and CT10 groups showed basically the same rule as Figure 5, while the SF10 group showed much higher strength than the other four groups in the three curing periods. In addition, because steam-curing can promote the hydration process, the strength of the JZ-2 group is significantly higher than that of the JZ-1. There was no significant difference in the strength of the JZ-2 group between 7 d and 28 d steam-curing. The results indicated that the hydration of the cement was almost complete after 7 days of steam-curing. The strength of the FT10 group, MT10 group, and CT10 group only increased slightly from

7 days to 28 days of steam-curing, indicating that tuff powder has low pozzolana effect. From the point of view of the strength analysis, compared with the FA, the MT and FT could contribute a higher cement mortar strength in the early, middle, and late periods, but they were still far lower than that of the SF.

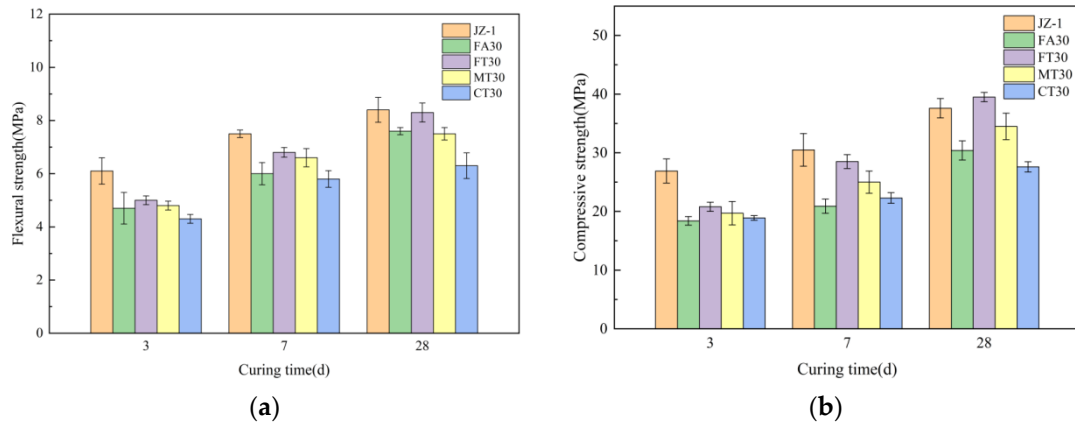


**Figure 5.** Strength of cement mortar for feasibility study of replacing fly ash. (a) Flexural strength; (b) compressive strength.

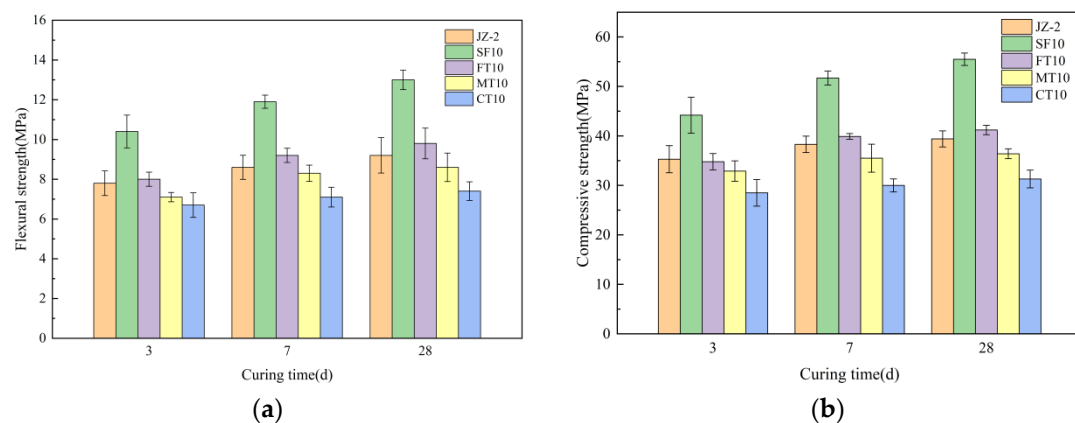


**Figure 6.** Strength of cement mortar for feasibility study of replacing silica fume. (a) Flexural strength; (b) compressive strength.

### 3.2. Fluidity

Fluidity is an important index to characterize the working performance of concrete. In this paper, the fluidity was characterized by testing the flow degree of the mortar. The fluidity of the mortar with different mix proportions are shown in Figures 7 and 8. It can be seen from the figures that the addition of the tuff powder and silica fume could reduce the fluidity of the mortar, and the smaller the particle size, the more obvious the reduction. The FT30 group decreased by 11.4% compared with the JZ-1 group, and the SF10 group decreased by 9% compared with the JZ-2 group. The addition of the fly ash could greatly improve the fluidity of the mortar, and the FA30 group was 15.2% higher than the JZ-1 group.

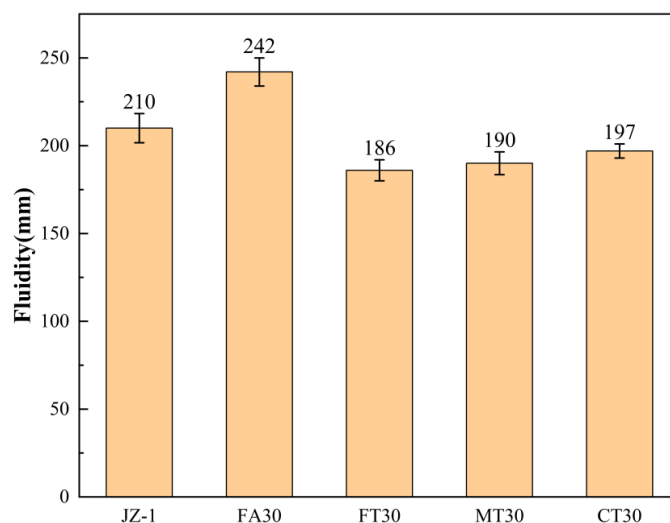


Figure 7. Fluidity of cement mortar for feasibility study of replacing fly ash.

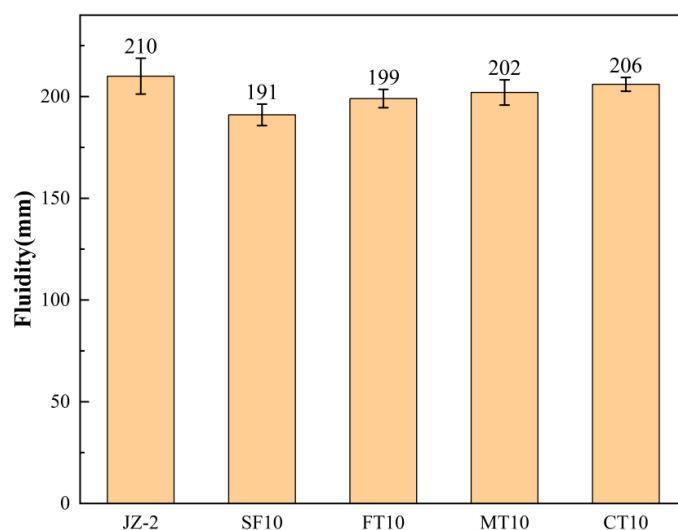


Figure 8. Fluidity of cement mortar for feasibility study of replacing silica fume.

### 3.3. Composition Analysis of Hydration Products

Through XRD patterns, it can be seen how much of each component is in the sample after 28 days of curing. The comparison of the XRD patterns with different cementation material systems at 28 days curing time are shown in Figures 9 and 10, respectively. Unreacted cement clinker (Alite and Ferrite), calcium hydroxide (Portlandite) generated by hydration reaction, and quartz (Quartz) in the cementing material were detected in all the specimens. In addition, since the amount of Aft and AFm generated by the hydration reaction was small, and C-S-H was mainly a gel material without a diffraction peak, and no effective diffraction peaks of them were found. After 28 days of curing, no diffraction peaks of the other hydration products were found in the mineral composition analysis, indicating that no new hydration products were formed after the tuff powder was incorporated into the cementitious system.

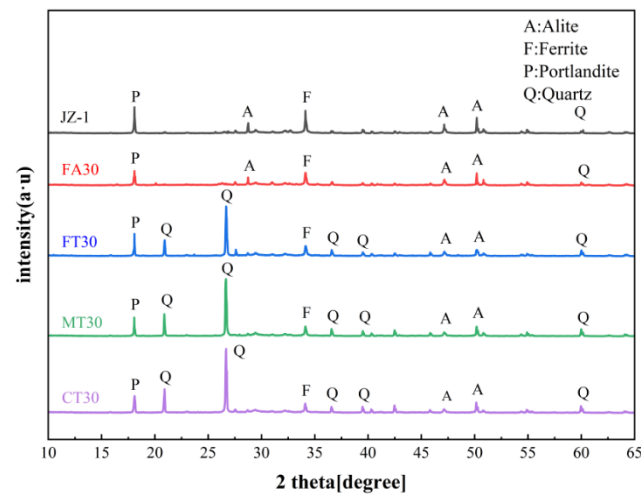


Figure 9. XRD patterns of the feasibility study group specimens for replacing fly ash at 28 days.

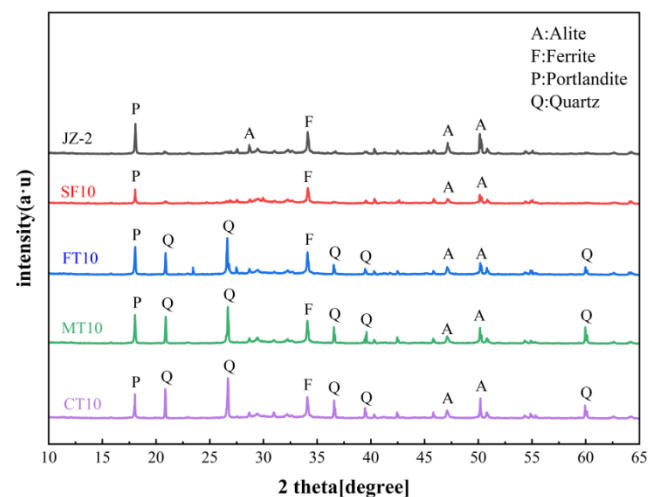


Figure 10. XRD patterns of the feasibility study group specimens for replacing silica fume at 28 days.

The XRD patterns of JZ-1, FA30, FT30, MT30, and CT30 at 28 days of curing are shown in Figure 9. It could be observed that the JZ-1 group had the highest amount of  $\text{Ca}(\text{OH})_2$ , which was generated by the hydration reaction between the cement clinker and water. This is due to the dilution effect caused by the addition of 30% different cementitious materials, resulting in a decrease in the total amount of the cement in the other four groups, causing the JZ-1 group to contain the highest amount of  $\text{Ca}(\text{OH})_2$ . The fly ash in the FA30 group had a certain amount of  $\text{Al}_2\text{O}_3$  and  $\text{SiO}_2$  which had certain pozzolanic activity and could react with the  $\text{Ca}(\text{OH})_2$  produced by the primary hydration reaction, resulting in a decrease in the content of  $\text{Ca}(\text{OH})_2$  in the FA30 group. The  $\text{Ca}(\text{OH})_2$  content of the FT30, MT30, and CT30 groups was higher than that of the FA30 group, and there was a high  $\text{SiO}_2$  diffraction peak. It could be seen that there was still a large amount of  $\text{SiO}_2$  in the tuff powder, indicating that the degree of the secondary hydration reaction was low. With the addition of the tuff powder, the content of  $\text{C}_3\text{S}$  in the FT30, MT30, and CT30 groups decreased, indicating that the tuff powder had the effect of nucleation, and the addition of the tuff powder could promote the hydration of the cement. In addition, with the decrease in particle size, the diffraction peak of  $\text{SiO}_2$  also gradually decreased, and more  $\text{SiO}_2$  participated in the secondary hydration reaction. Figure 10 shows the XRD pattern of the JZ-2, SF10, FT10, MT10, and CT10 groups at 28 days of curing. It can be found from the figure that the FT10, MT10, and CT10 groups showed the same rule as Figure 9, while the SF10 group had an extremely low content of  $\text{Ca}(\text{OH})_2$ , indicating that the silica fume had higher activity and could have a stronger secondary hydration reaction with  $\text{Ca}(\text{OH})_2$ . In

addition, since steam-curing can accelerate the hydration progress of the cement, the JZ-2 group has more  $\text{Ca(OH)}_2$  and less  $\text{C}_3\text{S}$  compared with the JZ-1 group.

### 3.4. DTG Analysis

The amount of  $\text{Ca(OH)}_2$  and other substances in each specimen can be obtained through the DTG weight loss curve. The DTG curves with different cementation material systems at 28 days curing time are shown in Figures 11 and 12, respectively. It can be seen that each curve has roughly the same trend, with the three obvious weight loss stages corresponding to the three obvious heat absorption peaks. The temperature range of the first stage is from room temperature to 300 °C. In the first stage C-S-H, the AFt and AFm products decomposed successively. The temperature range of the second stage is from 350 °C to 550 °C. In the second stage the  $\text{Ca(OH)}_2$  underwent dehydration and decomposition. The temperature range of the third stage is above 600 °C. In the third stage carbonates undergo dehydration and decomposition. As can be seen from Figure 11, in the first stage, the JZ-1, MT30, and FT30 groups had more weight loss, indicating that these three groups had more C-S-H gel content, while the FA30 and CT30 groups had less loss, indicating that the C-S-H gel content was less in these two groups, which was corresponding to the 28 d compressive strength results. In the second stage, the content of the  $\text{Ca(OH)}_2$  in the JZ-1, FT30, MT30, CT30, and FA30 groups decreased successively, corresponding to the XRD pattern analysis. This is because fly ash has good pozzolanic activity and can react with  $\text{Ca(OH)}_2$ , making the content of the  $\text{Ca(OH)}_2$  in group FA30 the lowest. The tuff powder of the FT30 and MT30 groups is finer and has a stronger nucleation, which promotes the hydration of the cement to produce more  $\text{Ca(OH)}_2$ , while the CT has lower nucleation, which promotes the hydration of the cement weakly, causing the CT30 group to have less  $\text{Ca(OH)}_2$  and C-S-H gel content. As can be seen from Figure 12, in the first stage, the SF10 group had a larger weight loss compared with the other four groups, indicating that the SF10 group had a higher C-S-H gel content. In the second stage, the  $\text{Ca(OH)}_2$  content in the JZ-2, FT10, MT10, CT10, and SF10 groups decreased successively, corresponding to the XRD phase pattern. This is because silica fume has a large amount of amorphous  $\text{SiO}_2$ , which can react with  $\text{Ca(OH)}_2$ , so its  $\text{Ca(OH)}_2$  content is the lowest. The variation rules of the FT10, MT10, and CT10 were similar to those of the FT30, MT30, and CT30.

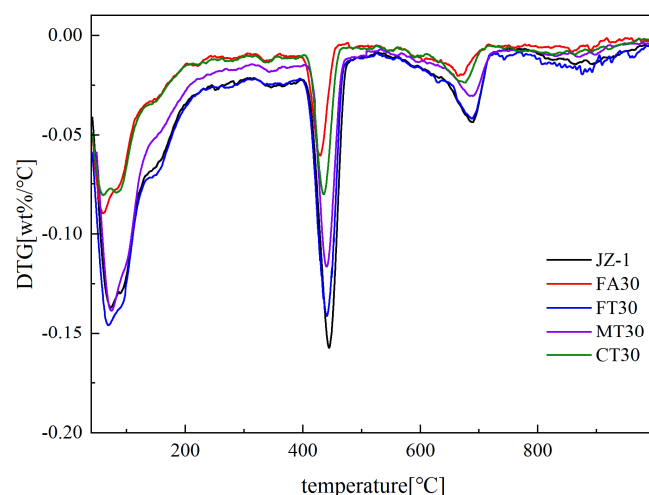


**Figure 11.** DTG patterns of the feasibility study group specimens for replacing fly ash at 28 days.

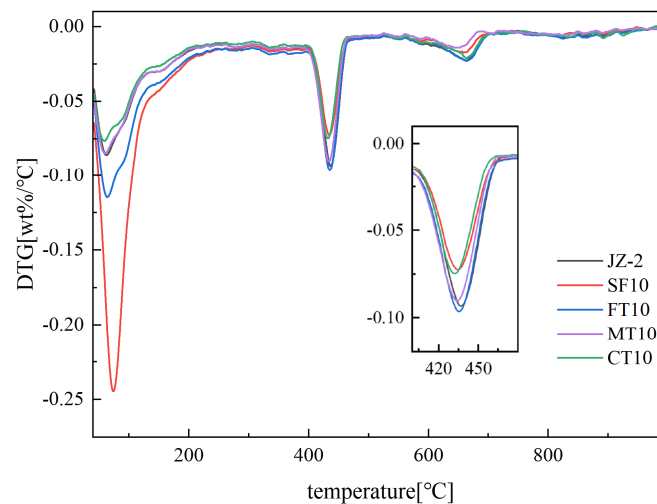


**Figure 12.** DTG patterns of the feasibility study group specimens for replacing silica fume at 28 days.

### 3.5. EDS Energy Spectrum Analysis

By EDS analysis of the specimens of each group, the content of each element can be detected, and the secondary hydration degree can be analyzed. At present, it has been found that the Ca/Si of the C-S-H gel has a great influence on the mechanical properties of the concrete. When the degree of the secondary hydration increases, the Ca element in the concrete will be consumed more, resulting in a decrease in the Ca/Si, an increase in the chain length in the C-S-H gel, and an enhancement of the micromechanical properties [25]. Figure 13 shows the EDS energy spectrum of the JZ-1, FA30, FT30, MT30, and CT30, and Table 7 shows the element content of each group specimens. It can be seen from Figure 13 and Table 7 that the Ca/Si of the JZ-1, CT30, MT30, FT30, and FA30 groups decreased successively, indicating the FA, FT, MT, and CT could all perform the secondary hydration reaction with the  $\text{Ca}(\text{OH})_2$ . The Ca/Si of FA30 was 1.20, and the Ca/Si of the FT30, MT30, and CT30 groups were 1.82, 1.72, and 1.63, respectively, indicating the secondary hydration degree of the tuff powder was low compared with FA. With the decrease in the tuff powder particle size, the Ca/Si increased, and the secondary hydration degree also kept increasing.

**Table 7.** EDS elemental analysis table of each group specimens at 28 days (At%).

	O	Na	Mg	Al	Si	K	Ca	Fe	Ca/Si
JZ-1	57.21	0.27	1.02	1.69	12.86	0.92	25.28	0.75	1.96
FA30	64.36	0.23	0.29	2.12	14.55	0.62	17.46	0.35	1.20
FT30	61.85	0.22	0.38	1.62	13.18	0.54	21.56	0.64	1.63
MT30	60.31	0.33	0.85	1.33	13.07	0.74	22.48	0.90	1.72
CT30	60.52	0.24	0.99	1.10	12.82	0.61	23.34	0.38	1.82

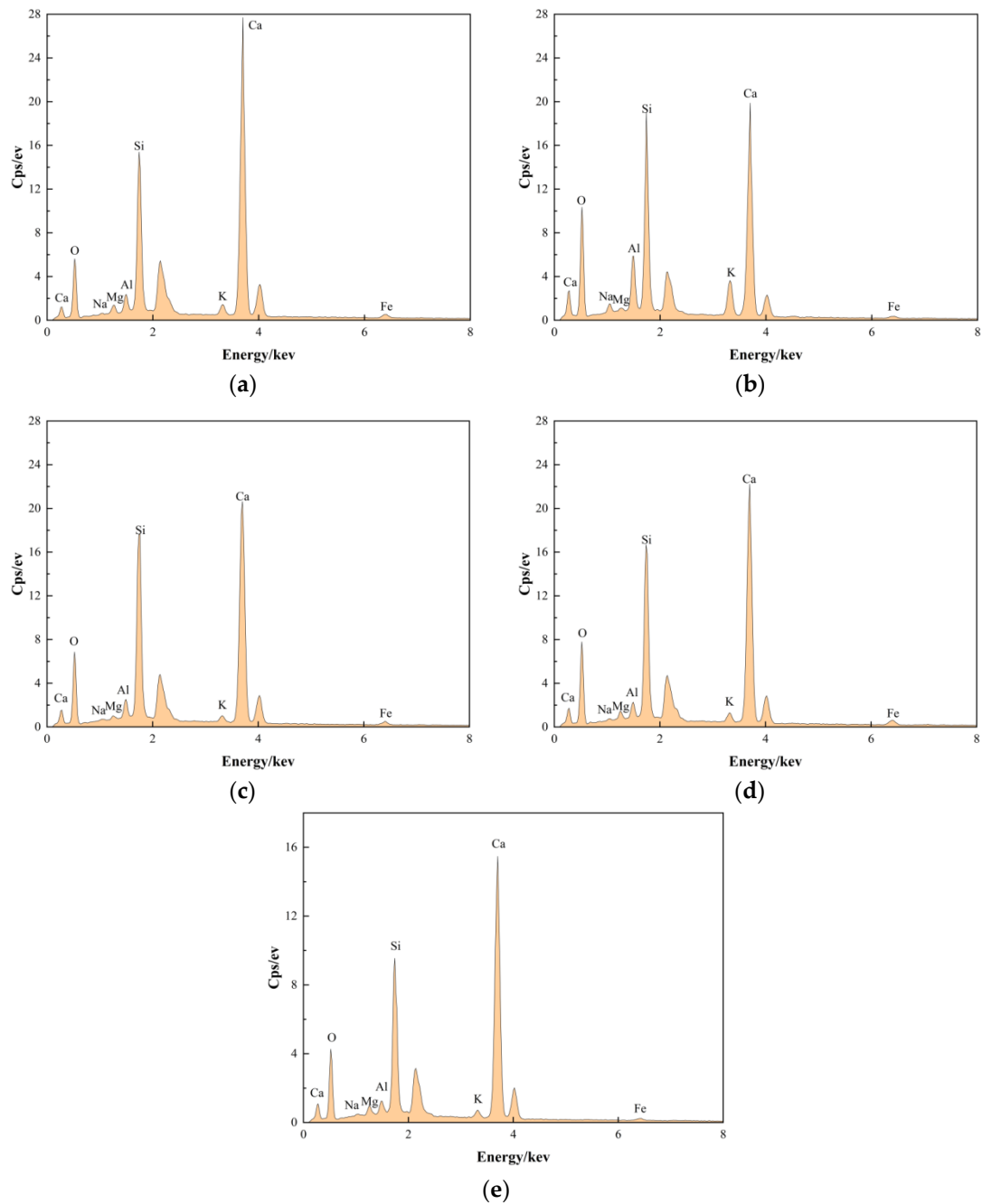


**Figure 13.** EDS energy spectrum of each group specimens at 28 days. (a) JZ-1; (b) FA30; (c) FT30; (d) MT30; (e) CT30.

## 4. Discussion

### 4.1. The Hydration Mechanism of Tuff Powder

Based on the results of this experiment, the hydration mechanism of replacing fly ash or silica fume with tuff powder was discussed. As shown in Figure 14, the primary functions of the tuff powder in the concrete are evidenced through the following three aspects: pozzolanic effect, nucleation effect, and filling effect. The nucleation effect and filling effect play a crucial role.

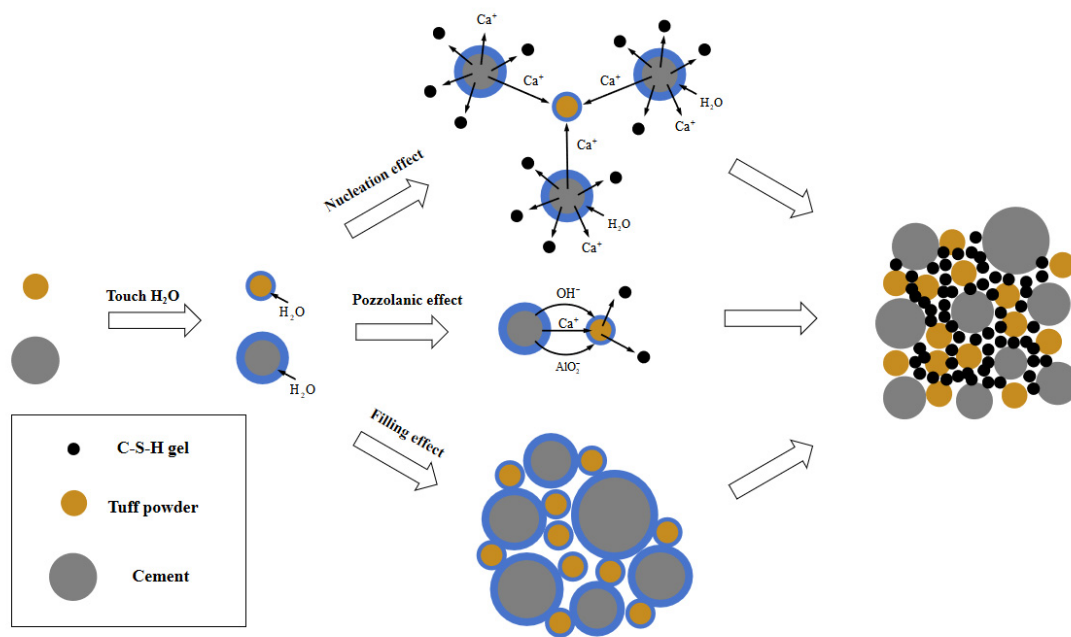


**Figure 14.** Action mechanism of tuff powder.

The analysis of the experimental results revealed that the tuff powder utilized in this study, despite its high  $\text{SiO}_2$  content, exhibited high crystallinity, thereby not undergoing secondary hydration reactions. Furthermore, the EDS spectroscopy at 28 days indicated a higher Ca/Si ratio in the concrete, implying a weaker volcanic ash activity. The XRD and DTG tests showed that the  $\text{C}_3\text{S}$  decreased and the C-S-H gel increased in the MT and FT groups compared with the FA group. This is due to the high specific surface area of tuff powder, which makes it have a relatively significant nucleation effect. The  $\text{Ca}^{2+}$  released during  $\text{C}_3\text{S}$  hydration can be adsorbed on the surface, weakening the oriented growth of the  $\text{Ca}(\text{OH})_2$  in the weak interface transition zone, providing nucleation points for hydration products, promoting the precipitation of the cement hydration products, and accelerating the formation of the C-S-H gel [26,27]. The FT can fill the interstice in the composite cementitious system, reduce the porosity in the system, improve the density, and thus increase the strength of the cement mortar [28,29]. In addition, the finer the tuff powder particles, the lower the  $\text{SiO}_2$  content in the 28d hydration products; this is because the finer the tuff powder particles, the faster the ion precipitation, the faster the secondary hydration reaction rate, so that more  $\text{SiO}_2$  can be consumed [4].

The finer the tuff powder particles, the less  $\text{C}_3\text{S}$  and the more  $\text{Ca}(\text{OH})_2$  were present in the 28 days hydration products of the cement mortar. This is because the ground tuff powder has a higher specific surface area, stronger adsorption capacity for  $\text{Ca}^{2+}$ , and stronger nucleation effect. Therefore, grinding can improve the strength of the specimens with tuff powder. In summary, the high activity of the tuff powder in the cement-based materials is due to the joint action of the nucleation effect, filling effect, and pozzolanic effect, but the nucleation effect and filling effect are the dominant factors.

The feasibility of replacing fly ash or silica fume with tuff powder was studied by measuring the mechanical properties and working properties of different cementitious systems mortar, respectively. It was found by XRD that the  $\text{Ca}(\text{OH})_2$  content in the FA30 and SF10 groups was lower, which was due to the fact that the fly ash and silica fume contained more active substances. The amorphous glass structure composed of silica tetrahedron and aluminum tetrahedron in fly ash can conduct a secondary hydration reaction with  $\text{Ca}(\text{OH})_2$  [30], thus improving the strength of the concrete, making the strength of the FA group higher than that of the CT group. Although the secondary hydration degree of group FA30 was higher, it did not show higher mechanical properties. This is because the mechanical properties of cement mortar are not only related to the secondary hydration

degree of the cementitious material, but also determined by the filling and nucleation effect of the cementitious material. Therefore, although the secondary hydration degree of the MT30 and FT30 groups were low, they could show high mechanical properties. Silica fume contains a large amount of amorphous  $\text{SiO}_2$ , which can continue to conduct secondary hydration reaction with  $\text{Ca}(\text{OH})_2$  produced by primary hydration to generate a large amount of low-calcium C-S-H gel, which greatly improves the density of cement mortar [31,32], and makes important contributions to the compressive strength and flexural strength, making the strength of the SF10 group much higher than that of the other groups.

#### *4.2. Analysis of the Influence of Tuff powder on Workability*

For work performance, due to the high specific surface area of tuff powder and silica fume, which can adsorb free water in mortar, the fluidity of mortar is reduced. Compared to tuff powder, silica fume has a more significant reduction in the fluidity of mortar. Fly ash contains a large number of smooth spherical particles, which can act as a “ball bearing” in concrete, reducing the friction force of concrete and improving its fluidity [33]. In summary, through the comprehensive consideration of the mechanical properties and working performance and other indicators, as auxiliary cementitious materials, MT and FT can completely replace fly ash in remote areas where materials are short, but cannot replace silica fume. When replacing fly ash, additional measures need to be taken to ensure the working performance of the concrete.

#### *4.3. Feasibility Analysis of Replacing Cement with Tuff Powder Partially*

As a kind of pozzolanic material, tuff is widely distributed in various parts of China, especially in western regions such as Luo village, Waka area, the Sangri County of Xizang Province, the Yining area of Xinjiang Province, and the Tianshui area of Gansu Province. The Xizang Gaozheng Building Materials Company has found a large number of tuff mines in Tibet, and the mineral reserves are extremely rich. In addition, the mining and processing procedures of tuff powder are simple. The raw tuff can be obtained by explosive means, and then the tuff powder can be obtained by crushing and grinding. If tuff powder is used as auxiliary cementitious material in concrete, it can effectively alleviate the shortage of concrete materials and the difficulty of transportation, so as to greatly reduce the cost of concrete construction in western China. According to the strength analysis, it can be seen that when the cement is replaced by tuff powder partially, the mortar has a considerable strength index. Although there is a big difference between the mortar of the tuff powder group and the benchmark group in the early and middle stages, the flexural strength and compressive strength of the tuff powder group in the late stage are slightly lower than the benchmark group, while the flexural strength of the FT group is close to the benchmark group, and the compressive strength is even higher than the benchmark group. However, because the surface of tuff is rough and porous and tuff has a high specific surface area, the fluidity of the cement mortar of the tuff powder group is significantly reduced compared with that of the benchmark group, and the finer the particle size of the tuff powder, the more obvious the decrease in fluidity. Therefore, when replacing cement with tuff powder, necessary measures should be taken to ensure the working performance under the premise of ensuring the strength.

## **5. Conclusions**

In order to study whether it is feasible for tuff powder to replace fly ash or silica fume, the following conclusions are obtained through the strength testing, hydration product phase analysis, DTG analysis, and EDS analysis of cement mortar mixed with different types of cementitious materials:

- (1) The specimens mixed with the MT and FT had high flexural and compressive strength in the early, middle, and later curing stages. Even in the later stage, the compressive strength of the specimens mixed with the FT was slightly higher than that of the benchmark group, while the specimens mixed with the CT had lower strength in the

early, middle, and later curing stages. Further grinding could be used to reduce the particle size of tuff powder, improve its activity, and enhance its contribution to the strength of cement mortar. In addition, the strength of the specimens doped with the MT and FT were higher than that of the specimens doped with the fly ash, but much lower than that of the specimens doped with the silica fume.

- (2) Due to the fact that tuff powder has a high specific surface area, the addition of the tuff powder reduced the fluidity of the cement mortar, and the smaller the particle size, the more obvious the fluidity reduction. The fluidity of the cement mortar was greatly reduced by silica fume. The addition of the fly ash improved the fluidity of the cement mortar.
- (3) Through the phase analysis of hydration products, it was found that no new hydration products were generated after the addition of the tuff powder. Due to the nucleation effect, the addition of the tuff powder would promote the primary hydration of the cement, and the smaller the particle size, the stronger the promotion degree, resulting in the decrease in  $C_3S$  and the increase in  $Ca(OH)_2$  and C-S-H gel content.
- (4) Compared with fly ash, the ability of the tuff powder to participate in the secondary hydration reaction was weak, and the ability of the coarse-particle-size tuff powder was weaker. The high activity of tuff powder in cement-based materials is due to the joint action of nucleation effect, filling effect, and pozzolanic effect, but the nucleation and filling effect are the dominant factors.
- (5) In remote areas where materials are short, medium-particle-size tuff powder and fine-particle-size tuff powder can completely replace fly ash, but cannot replace silica fume as auxiliary cementing materials. When replacing fly ash, additional measures should be required to ensure the performance of the concrete.

**Author Contributions:** Conceptualization, T.L. and Z.W.; methodology, T.L. and B.L.; software, T.L.; validation, T.L., Z.Z. and L.L.; formal analysis, Q.N.; investigation, T.L.; resources, L.L.; data curation, Z.W.; writing—original draft preparation, T.L.; writing—review and editing, Z.Z.; visualization, L.L.; supervision, T.L.; project administration, Z.W.; funding acquisition, Z.W. All authors have read and agreed to the published version of the manuscript.

**Funding:** This research was funded by “Research and development of low carbon high performance concrete materials and its application technology in plateau wading environment” grant number “2023YFQ0047”.

**Data Availability Statement:** The original contributions presented in the study are included in the article, further inquiries can be directed to the corresponding author.

**Conflicts of Interest:** The authors declare no conflict of interest.

## References

1. Kinnunen, P.; Sreenivasan, H.; Cheeseman, C.R.; Illikainen, M. Phase separation in alumina-rich glasses to increase glass reactivity for low- $CO_2$  alkali-activated cements. *J. Clean. Prod.* **2019**, *213*, 126–133. [[CrossRef](#)]
2. Edris, W.F.; Abdelkader, S.; Salama, A.H.E.; Al Sayed, A.A.-K.A. Concrete Behaviour with Volcanic Tuff Inclusion. *Civ. Eng. Archit.* **2021**, *9*, 1434–1441. [[CrossRef](#)]
3. Yuan, Q.; Yang, Z.Z.; Shi, C.J.; Tan, Y.B.; An, X.P. Fundamentals on application of Natural pozzolans in cement-based materials: A review. *Bull. Chin. Ceram. Soc.* **2020**, *39*, 2379–2392.
4. Liu, S.; Fang, P.; Wang, H.; Kong, Y.; Ouyang, L. Effect of tuff powder on the hydration properties of composite cementitious materials. *Powder Technol.* **2021**, *380*, 59–66. [[CrossRef](#)]
5. DL/T 5273-2012; Technical Specification of Natural Pozzolan for Use in Hydraulic Concrete. State Quality Supervision Bureau: Beijing, China, 2012.
6. Mu, S.C. Physical and chemical features of tuff and its development and application. *China Min. Mag.* **2000**, *9*, 20–23.
7. Wang, Z.; Li, H.J.; Hang, F.L.; Tao, J.Q.; Sun, D.E.; Yi, Z.L.; Xie, Y.J. Fluidity and Mechanical Properties of Cement Mortar with Different Lithological Powders. *Bull. Chin. Ceram. Soc.* **2019**, *38*, 1585–1590.
8. Zhang, H.C.; Ji, X.X.; Tang, F.Y.; Wang, Y.; Chen, G.Q. Feasibility Study on Tuff Stone Powder as Concrete Admixture. *Constr. Technol.* **2017**, *46* (Suppl. S1), 282–285.
9. Shi, Y.; Li, X.; Li, Y.; Peng, Z.; Li, J. Effect of Tuff Powder Mineral Admixture on the Macro-Performance and Micropore Structure of Cement-Based Materials. *Front. Mater.* **2020**, *7*, 595997. [[CrossRef](#)]

10. Peng, S.; Li, X.; Wu, Z.; Chen, J.; Lu, X. Study of the key technologies of application of tuff powder concrete at the Daigo hydropower station in Tibet. *Constr. Build. Mater.* **2017**, *156*, 1–8. [[CrossRef](#)]
11. Guo, S.M. Application and research of PT double admixture in Dachaoshan roller compacted concrete gravity dam. *Yunnan Water Power* **2000**, *3*, 19–23.
12. Çavdar, A.; Yetgin, Ş. Availability of tuffs from northeast of Turkey as natural pozzolan on cement, some chemical and mechanical relationships. *Constr. Build. Mater.* **2007**, *21*, 2066–2071. [[CrossRef](#)]
13. Kupwade-Patil, K.; Al-Aibani, A.F.; Abdulsalam, M.F.; Mao, C.; Bumajdad, A.; Palkovic, S.D.; Büyüköztürk, O. Microstructure of cement paste with natural pozzolanic volcanic ash and Portland cement at different stages of curing. *Constr. Build. Mater.* **2016**, *113*, 423–441. [[CrossRef](#)]
14. Ababneh, A.; Matalkah, F. Potential use of Jordanian volcanic tuffs as supplementary cementitious materials. *Case Stud. Constr. Mater.* **2018**, *8*, 193–202. [[CrossRef](#)]
15. Biricik, H.; Karapinar, L.S. Pozzolanic activity of central Anatolian volcanic tuff and its usability as admixture in mortar. *Adv. Cem. Res.* **2018**, *32*, 91–100. [[CrossRef](#)]
16. Turanlı, L.; Uzal, B.; Bektas, F. Effect of large amounts of natural pozzolan addition on properties of blended cements. *Cem. Concr. Res.* **2005**, *35*, 1106–1111. [[CrossRef](#)]
17. Cao, X.; Xia, D.C.; Yin, W.X.; Jiang, L.H.; Zhang, Y. The influence of tuffaceous rock powder and VF anti cracking agent on the hydration characteristics of cement slurry. *Hong Shui River* **2016**, *35*, 38–41, 58.
18. Li, H.; Wang, Z.; Sun, R.; Huang, F.; Yi, Z.; Yuan, Z.; Wen, J.; Lu, L.; Yang, Z. Effect of different lithological stone powders on properties of cementitious materials. *J. Clean. Prod.* **2021**, *289*, 125820. [[CrossRef](#)]
19. GB 8076-2008; Concrete Admixture. State Quality Supervision Bureau: Beijing, China, 2008.
20. JB/T 315-2011; Natural Pozzolanic Materials Used for Cement Mortar and Concrete. State Quality Supervision Bureau: Beijing, China, 2011.
21. GB/T 27690-2023; Silica Fume for Mortar and Concrete. State Quality Supervision Bureau: Beijing, China, 2023.
22. GB/T 17671-2021; Test Method of Cement Mortar Strength (ISO Method). State Quality Supervision Bureau: Beijing, China, 2021.
23. GB/T 2419-2005; Test Method for Fluidity of Cement Mortar. State Quality Supervision Bureau: Beijing, China, 2005.
24. Shi, C.; Yuan, Q. *Test and Analysis Methods for Cement-Based Materials*, 1st ed.; China Building Industry Press: Beijing, China, 2018; pp. 166–168.
25. Wang, J.; Hu, Z.; Chen, Y.; Huang, J.; Ma, Y.; Zhu, W.; Liu, J. Effect of Ca/Si and Al/Si on micromechanical properties of C(-A)-S-H. *Cem. Concr. Res.* **2022**, *157*, 106811. [[CrossRef](#)]
26. Bentz, D.P. Modeling the influence of limestone filler on cement hydration using CEMHYD3D. *Cem. Concr. Compos.* **2006**, *28*, 124–129. [[CrossRef](#)]
27. Bonavetti, V.L.; Rahhal, V.F.; Irassar, E.F. Studies on the carboaluminate formation in limestone filler-blended cements. *Cem. Concr. Res.* **2001**, *31*, 853–859. [[CrossRef](#)]
28. Shi, C.J.; Wang, D.H.; Jia, H.F.; Liu, J.H. Role of Limestone Powder and Its Effect on Durability of Cement-Based Materials. *Bull. Chin. Ceram. Soc.* **2017**, *45*, 1582–1593.
29. Lu, X.; Pei, L.; Peng, S.; Li, X.; Chen, J.; Chen, C. Hydration, Hardening Mechanism, and Performance of Tuff Normal Concrete. *J. Mater. Civ. Eng.* **2021**, *33*, 04021063. [[CrossRef](#)]
30. Jiang, T.H.; Guan, J.C.; Zhang, X.C. Summary of Application of Admixtures in Ultra-High Performance Concrete. *Sci. Technol. Eng.* **2022**, *22*, 5528–5538.
31. Yazıcı, H.; Yiğiter, H.; Karabulut, A.Ş.; Baradan, B. Utilization of fly ash and ground granulated blast furnace slag as an alternative silica source in reactive powder concrete. *Fuel* **2008**, *87*, 2401–2407. [[CrossRef](#)]
32. Zhang, W.; Zhang, Y.; Liu, L.; Zhang, G.; Liu, Z. Investigation of the influence of curing temperature and silica fume content on setting and hardening process of the blended cement paste by an improved ultrasonic apparatus. *Constr. Build. Mater.* **2012**, *33*, 32–40. [[CrossRef](#)]
33. Xu, H.Y.; Sha, J.F.; Liu, J.Z.; Lu, J.Y.; Go, F. Research on the influence and evaluation method of fly ash on the flowability of cement-based materials. *China Concr. Cem. Prod.* **2014**, *12*, 5–8.

**Disclaimer/Publisher’s Note:** The statements, opinions and data contained in all publications are solely those of the individual author(s) and contributor(s) and not of MDPI and/or the editor(s). MDPI and/or the editor(s) disclaim responsibility for any injury to people or property resulting from any ideas, methods, instructions or products referred to in the content.